Human Molecular Genetics, 2019, Vol. 28, No. 3 386–395

doi: 10.1093/hmg/ddy341
Advance Access Publication Date: 25 September 2018
General Article

GENERAL ARTICLE

Mice lacking α-, β1- and β2-syntrophins exhibit diminished function and reduced dystrophin expression in both cardiac and skeletal muscle

Min Jeong Kim, Nicholas P. Whitehead, Kenneth L. Bible, Marvin E. Adams* and Stanley C. Froehner

Department of Physiology and Biophysics, University of Washington, Seattle, WA 98195, USA

*To whom correspondence should be addressed at: 1705 Pacific ST NE Rm G424 HSB Seattle, WA 98195-7290, USA. Tel: 206 543 9094; Fax: 206 685 0619; Email: marva@uw.edu

Abstract

Syntrophins are a family of modular adaptor proteins that are part of the dystrophin protein complex, where they recruit and anchor a variety of signaling proteins. Previously we generated mice lacking α- and/or β2-syntrophin but showed that in the absence of one isoform, other syntrophin isoforms can partially compensate. Therefore, in the current study, we generated mice that lacked α, β1 and β2-syntrophins [triple syntrophin knockout (tKO) mice] and assessed skeletal and cardiac muscle function. The tKO mice showed a profound reduction in voluntary wheel running activity at both 6 and 12 months of age. Function of the tibialis anterior was assessed *in situ* and we found that the specific force of tKO muscle was decreased by 20–25% compared with wild-type mice. This decrease was accompanied by a shift in fiber-type composition from fast 2B to more oxidative fast 2A fibers. Using echocardiography to measure cardiac function, it was revealed that tKO hearts had left ventricular cardiac dysfunction and were hypertrophic, with a thicker left ventricular posterior wall. Interestingly, we also found that membrane-localized dystrophin expression was lower in both skeletal and cardiac muscles of tKO mice. Since dystrophin mRNA levels were not different in tKO, this finding suggests that syntrophins may regulate dystrophin trafficking to, or stabilization at, the sarcolemma. These results show that the loss of all three major muscle syntrophins has a profound effect on exercise performance, and skeletal and cardiac muscle dysfunction contributes to this deficiency.

Introduction

Syntrophins are a family of 58–60 kDa proteins consisting of five isoforms (α, β1, β2, γ1 and γ2) encoded by separate genes. Structurally, syntrophins contain one postsynaptic density protein-95/disc large/zona occludens-1 (PDZ) domain, two pleckstrin homology (PH) domains and a syntrophin unique (SU) domain at the carboxyl terminus (1). α-, β1- and β2-syntrophins have multiple binding motifs and directly bind to dystrophin, utrophin and dystrobrevin via the PH2-SU region (2–5). In mouse skeletal muscle, γ2-syntrophin is not associated with dystrophin but instead is localized to the endoplasmic reticulum (6). γ1-syntrophin is not expressed in skeletal muscle or heart.

An important function of muscle syntrophins is to bind signaling proteins and localize them to the sarcolemma via interaction with dystrophin, the protein product of the Duchenne

Received: June 11, 2018. **Revised:** August 21, 2018. **Accepted:** September 21, 2018

muscular dystrophy locus. Syntrophins use their PDZ domains to bind a variety of channels, pumps and signaling proteins, including aquaporin 4 (AQP4) (7), sodium channel (SCN5A) (8), calcium pump (PMCA4B) (9), nNOS (10–12) and serine/threonine kinases (13,14). For a complete list of proteins that bind syntrophins, see the review by Allen *et al.* (15). Syntrophins also interact with phospholipids via the PH domains (16). α-syntrophin is the predominant isoform in skeletal and cardiac muscle and is also expressed at a lower level in the brain. β1-Syntrophin is expressed on the sarcolemma of skeletal muscle fast fibers and β2-syntrophin is expressed primarily at the neuromuscular junction (NMJ) (17–19). α -Syntrophin is also the dominant syntrophin isoform in cardiac muscle where it forms a complex with, nNOS, PMCA4B and SCN5A (20).

Previously, we characterized the neuromuscular morphology and function of mice lacking single syntrophin isoforms (αKO or β2KO) as well as the double knockout (α/β2KO) mice (21,22). There is no obvious myopathy in αKO mice despite reductions in nNOS and α-dystrobrevin2 expression. This may be at least partially due to an upregulation of β1- and β2-syntrophins in the absence of α-syntrophin (21). At the NMJ postsynaptic membrane, expression of utrophin, acetylcholine receptor and acetylcholinesterase was reduced in αKO mice (21). β2KO showed normal NMJs and also did not display any signs of muscle myopathy (22). In contrast, α/β2KO mice showed more NMJ structural abnormalities compared with mice lacking only one syntrophin. Furthermore, the α/β2KO mice demonstrated a significant reduction of voluntary exercise activity not seen in the parent strains (22).

In the heart, very little is known about the roles of the various syntrophin isoforms on cardiac signaling and function. It has been reported that point mutations of α-syntrophin (A390V, A257G and E409Q) lead to long QT syndrome, due to α-syntrophin's interaction with the cardiac sodium channel SCN4A (23–26). It has also been reported that the composition of the dystrophin complex is different in skeletal and cardiac muscle. Cardiac muscle expresses more β1-syntrophin than skeletal muscle and more of the cardiac β2-syntrophin is bound to dystrophin than in skeletal muscle (27). However, the role(s) of α and β-syntrophins on cardiac function and cardiomyopathy has not been investigated.

In this study, we have evaluated the effects of removing all three major muscle syntrophin isoforms (tKO) on both skeletal and cardiac muscle function as well as voluntary exercise performance. We report that tKO mice show evidence of impaired function in both skeletal and cardiac muscle and display a profound reduction in voluntary exercise activity. We also reveal that loss of syntrophins leads to reduced expression of dystrophin at the sarcolemma, which provides new insights into the regulation of the dystrophin protein complex and its role in modulating muscle signaling and function.

Results

Generation and characterization of β1-syntrophin knockout mice

Previously, we generated and characterized the α-syntrophin knockout (αKO), the β2-syntrophin knockout (β2KO) and the α/β2 syntrophin double knockout (α/β2KO) mice (1,21,22). In those studies, we found that β1-syntrophin was upregulated in αKO muscle (21). To account for the possible compensatory effects of β1-syntrophin in αKO and α/β2 KO mice, we generated β1-syntrophin knockout mice (β1KO) (Fig. 1A). The absence of β1-syntrophin in β1KO mice was confirmed by western blots in liver and skeletal muscle from wild-type (WT) (+/+), heterozygous knockout (+/−) and homozygous knockout (−/−) mice (Fig. 1B). We used the liver as a positive control for β1-syntrophin since this isoform is highly expressed in liver (19). Interestingly, α-syntrophin was upregulated in liver and skeletal muscle from the β1KO. The β1KO mice showed no overt phenotype and showed no discernable muscle myopathy by histochemical techniques. We therefore cross-bred the β1KO mice with the α/β2KO mice to generate α/β1/β2 tKO mice in order to determine the physiological consequences of losing all major muscle syntrophin isoforms.

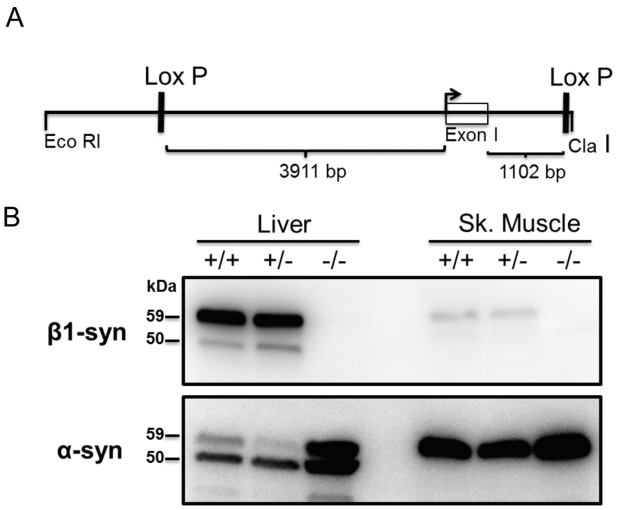

Figure 1. The structure of construct and protein expression in tissues of β1KO mice. **(A)** Generation and characterization of β1-syntrophin null mice. A construct containing loxP sites located before and after the first exon of β1-syntrophin was inserted into an ES cell line by homologous recombination. These cells were used to generate 'floxed' mice that were bred with mice expressing the CMV-Cre transgene to generated germline β1-syntrophin null mice. **(B)** Western blots of liver and skeletal muscle homogenates from mice bred with CMV-Cre verify that β1-syntrophin is not expressed in these mice. In the same homogenates, α-syntrophin is upregulated in the absence of β1-syntrophin.

Voluntary wheel running is significantly reduced in tKO mice

To evaluate whole body exercise performance, mice were caged individually with access to a voluntary wheel and revolutions were measured for 14 days at the ages of 6 months or 12–15 months (Fig. 2). At 6 months of age, relative to WT mice, average wheel revolutions were significantly reduced for both the αKO (64% of WT) and tKO (24% of WT) mice (Fig. 2A). There was also a significant difference between values for αKO and tKO at 6 months old (Fig. 2A). In 12- to 15-month-old mice, WT running wheel revolution reduced to 68% of 6-month-old values (Fig. 2A). 12- to 15-month-old αKO and tKO mice ran 35 and 32% as much as 6-month-old WT mice, respectively, with values for both groups significantly <12- to 15-month-old WT mice (Fig. 2A). Interestingly, at this age, the relative wheel revolutions of αKO and tKO mice were not significantly different. We plotted the daily wheel revolutions to see whether the running patterns were different in the three mouse strains. The daily average running revolutions of 12- to 15-month-old mice decreased in WT and αKO by 30 and 40% compared with 6 months old, while

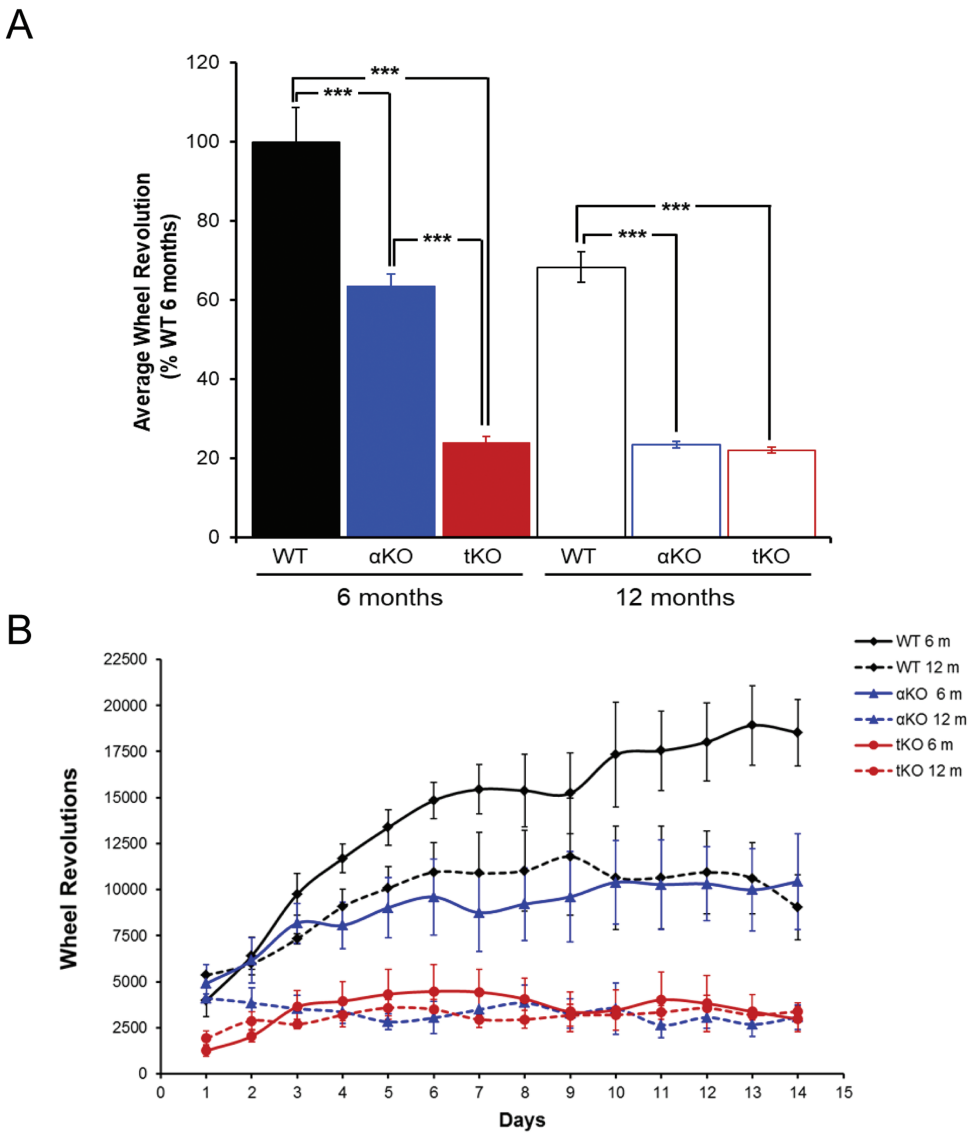

Figure 2. Knockout of three syntrophin isoforms reduced mice voluntary wheel running. **(A)** Average wheel revolutions for 14 days were calculated through relative values for WT 6 months. **(B)** Daily wheel revolutions during 14 days both in 6 and 12–15 months old. 6 months: WT ($n = 6$), αKO ($n = 6$), tKO ($n = 5$). 12–15 months: WT ($n = 4$), αKO ($n = 4$), tKO ($n = 6$) $^{***}P < 0.001$.

values for tKO mice, which had low activity levels at both time points, were similar at both time points (Fig. 2B).

Skeletal muscle *in situ* function is affected by absence of syntrophins

To determine whether the attenuated voluntary running performance in tKO mice was due to impaired skeletal muscle function, we measured *in situ* muscle force production in Tibialis Anterior (TA) muscles from WT and tKO mice. At 6 months of age, the specific force (isometric force normalized to cross-sectional area) of tKO mice was significantly less than WT mice by 20–25% over a range of stimulation frequencies (Fig. 3A). However, at 12–15 months of age, only the specific force at 80 Hz stimulation was significantly lower in tKO compared with WT, while values at 120 and 200 Hz were not different between the two groups (Fig. 3B). When comparing values at 6 and 12–15 months of age for each group, specific force decreased by 19% for WT and 9% for tKO.

Fiber-type distribution in skeletal muscle is altered by loss of syntrophins

We investigated if the specific force difference between tKO and WT was related to a change in the muscle fiber-type composition in tKO mice. Adult mammalian skeletal muscle expresses four major myosin heavy chain isoforms, one slow isoform (type 1) and three fast isoforms (type 2A, 2X and 2B) (28,29). Type 2B muscle fibers generate the highest specific force, while type 2X and 2A fibers generate intermediate force and type 1 fibers generate the lowest force (30). In TA muscle from the αKO and tKO, type 2A positive fibers increased about 8% compared to WT (Fig. 4A). The diaphragm muscle in αKO and tKO has significantly increased type 2A positive fibers (about 8 and 11%, respectively)

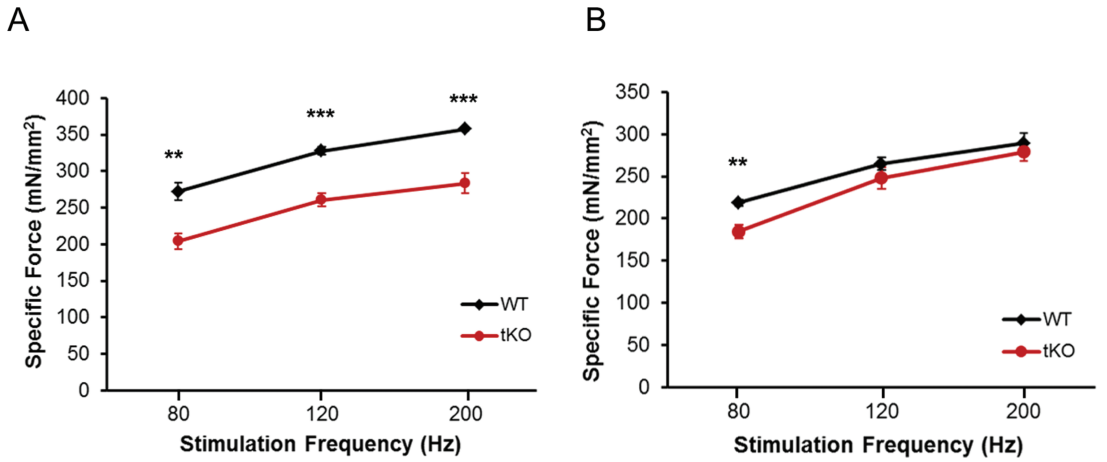

Figure 3. Knockout of three syntrophin isoforms reduces specific force generation of TA muscle. Specific force at various stimulation frequencies at the age of **(A)** 6-month-old for WT and tKO, and **(B)** 15-month-old WT ($n = 5$), tKO ($n = 5$) $^{**}P < 0.01$, $^{***}P < 0.001$.

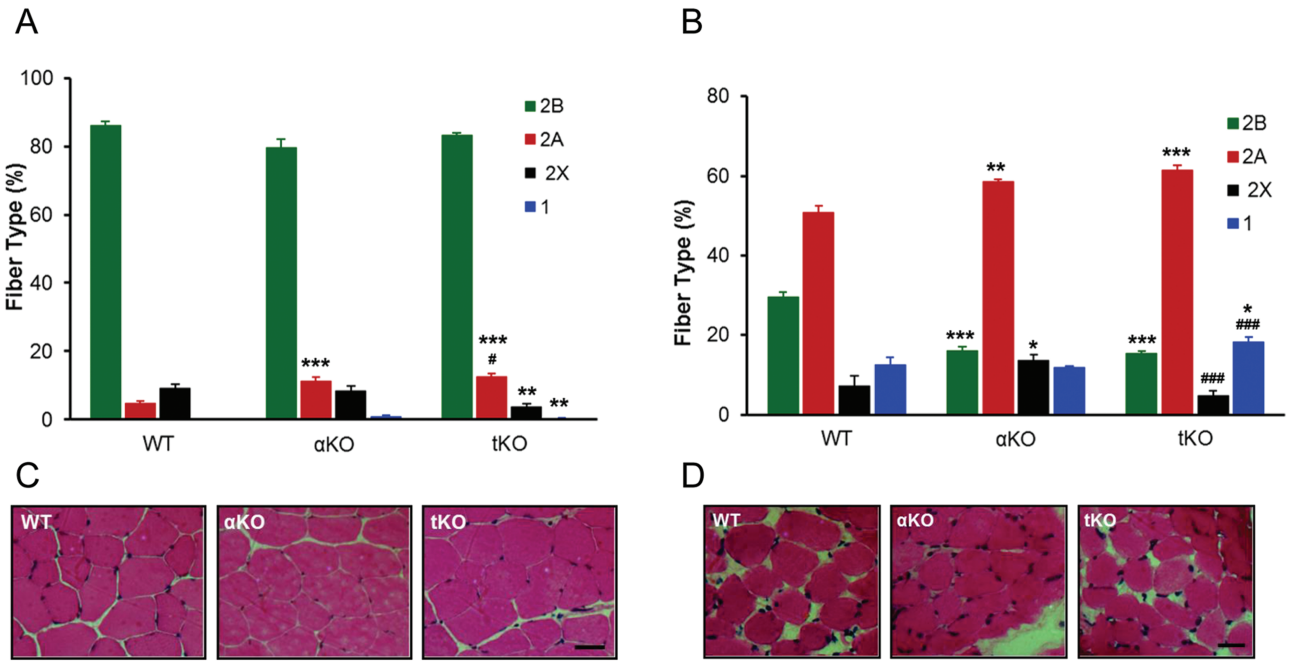

Figure 4. Fiber-type composition from the tKO mice showed more slow muscle fibers. **(A)** Fiber type in TA muscle from each mouse strain. WT ($n = 5$), αKO ($n = 4$), tKO ($n = 7$). **(B)** Fiber type in diaphragm from each mice $^{*}P < 0.05$ $^{**}P < 0.01$ $^{***}P < 0.001$ WT versus αKO and WT versus tKO, $^{\#}P < 0.05$ $^{\#\#\#}P < 0.001$ αKO versus tKO **(C)** representative H&E staining image cross section of TA **(D)** representative H&E staining of Diaphragm Scale bar = 50 μm.

and tKO show significant reduction in 2B fibers compared to WT (Fig. 4B). We also used these muscle sections to measure the levels of central nucleation, a marker of muscle regeneration following damage. We did not find any difference in the numbers of centrally nucleated fibers between WT, αKO and tKO both in TA and diaphragm muscle (Fig. 4C and D).

Cardiac function is impaired in syntrophin KO mice

Systolic and diastolic cardiac function in the absence of syntrophins has not been previously investigated. Therefore, we measured the cardiac function of WT, αKO and tKO *in vivo* by echocardiography at the ages of 3, 6 and 12 months. First, we measured left ventricular function using the myocardial performance index (MPI), a global index of the left ventricular systolic and diastolic function. Higher values of MPI indicate worsening left ventricular function. Both αKO and tKO showed significantly higher MPI at 3, 6, and 12 months of age compared to WT mice (Fig. 5A). We then aimed to determine whether the increased MPI was due to systolic and/or diastolic dysfunction. Systolic parameters, such as ejection fraction (EF) and fraction shortening (FS) were increased for tKO at 3, 6 and 12 months of age. αKO mice showed lower EF and FS at 3 months but higher than WT at 6 and 12 months old (Fig. 5C and D). Interestingly, the left ventricular posterior wall thickness during diastole (LVPW;d) was significantly greater in tKO mice at 3 (1.16 mm), 6 (1.27 mm) and 12 (1.23 mm) months of age compared to WT, while the LVPW;d of αKO was higher only at 12 month old (1.13 mm) mice compared to WT (Fig. 5B). The EF and FS were increased in tKO compared

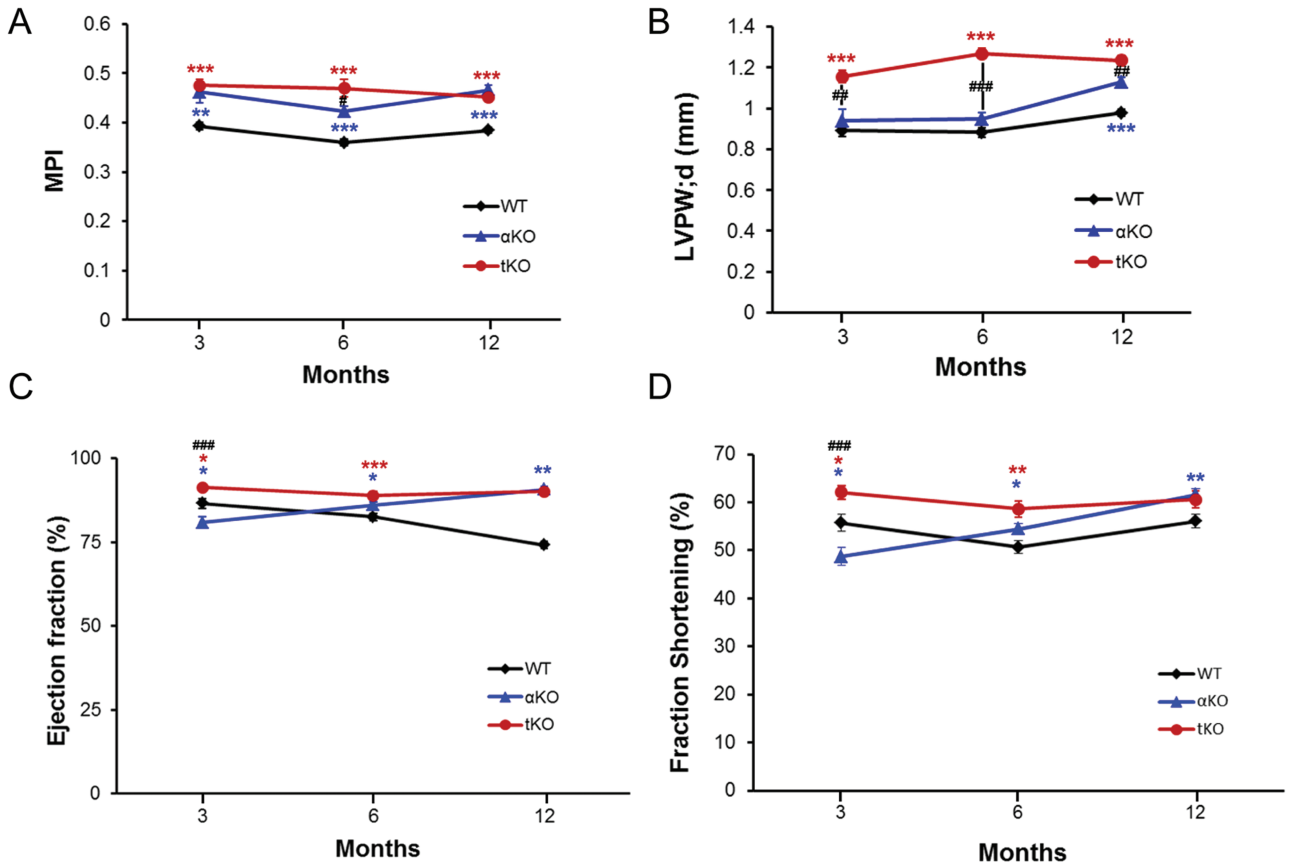

Figure 5. Knockout of three syntrophin isoforms induced systolic dysfunction and thickness of posterior wall in left ventricle. **(A)** MPI was measured from each mouse at the various age. **(B)** LVPW;d at various age of each mice group. **(C)** EF **(D)** Fractioning shortening calculated from each mice group at several age. $^{*}P < 0.05$ $^{**}P < 0.01$ $^{***}P < 0.001$. Red color, WT versus tKO; blue color, WT versus αKO; and $^{\#}P < 0.05$, $^{\#\#}P < 0.01$ $^{\#\#\#}P < 0.001$. αKO versus tKO, WT ($n = 16$), αKO ($n = 11$), tKO ($n = 14$).

to WT over the all measured time points (Fig. 5C and D). These results suggest that the tKO has a hypertrophic remodeling of the left ventricular wall, which leads to systolic cardiac dysfunction. Values obtained from echocardiography at each time point from the three mice strains are shown in Supplementary Material, Table S1.

Dystrophin expression at the sarcolemma is reduced in skeletal and cardiac muscles of tKO mice

Previously, α-dystrobrevin knockout mice showed less membrane associated dystrophin in heart (31). Since syntrophins bind α-dystrobrevin (19), in the present study we investigated whether localization and/or expression of dystrophin complex proteins were altered in syntrophin KO mice. To evaluate protein localization, we isolated ventricular cardiomyocytes from WT, αKO, β1KO and tKO mice and labeled for dystrophin, α-syntrophin, β1-syntrophin, nNOS, α-dystrobrevin1 and α-dystrobrevin2. The membrane localization of α-dystrobrevin1 and α-dystrobrevin2 in cardiomyocytes was reduced in αKO, as shown previously in skeletal muscle (21) and in tKO (Fig. 6). Interestingly, membrane-localized dystrophin levels were also significantly decreased in tKO cardiomyocytes and to a lesser extent in skeletal muscle (see Figs 6 and 7 and Supplementary Material Fig. S1). To obtain more quantitative data, expression levels of dystrophin associated proteins in skeletal and cardiac muscles from WT and tKO mice were determined by western blotting. Membrane-enriched and soluble cytoplasmic fractions were prepared from each muscle (32). As shown in Figure 7, the expression of α-dystrobrevin1 and α-dystrobrevin2 was significantly reduced in tKO skeletal and cardiac muscles in both the cytoplasmic and membrane fractions (Fig. 7A). The expression of nNOS in gastrocnemius muscle was reduced as predicted based on the absence of its binding protein α-syntrophin (12,32). Remarkably, dystrophin expression was significantly reduced in tKO skeletal and cardiac muscles compared to WT (see Fig. 7A). For tKO, membrane-localized dystrophin levels in cardiac and skeletal muscles were reduced to 27 and 59% of WT values, respectively (Fig. 7B). Since dystrophin mRNA transcript levels from cardiac and skeletal muscle were not significantly different between tKO and WT mice (Fig. 7C), our results suggest that the absence of all syntrophin isoforms reduces membrane-localized dystrophin through post-transcriptional mechanisms.

Discussion

While a number of studies have investigated the roles of individual syntrophin isoforms (4,13,17,21,32,33), functional compensation by upregulation of other isoforms can mask a phenotype. We have shown previously that in the absence of α-syntrophin, β1-syntrophin is upregulated in muscle (21). Furthermore, we have shown that the NMJ phenotype of the α/β2 syntrophin knockout (α/β2 KO) mouse is more severe than either the α-syntrophin or β2-syntrophin single knockouts suggesting some compensatory mechanisms are present. Therefore, in the

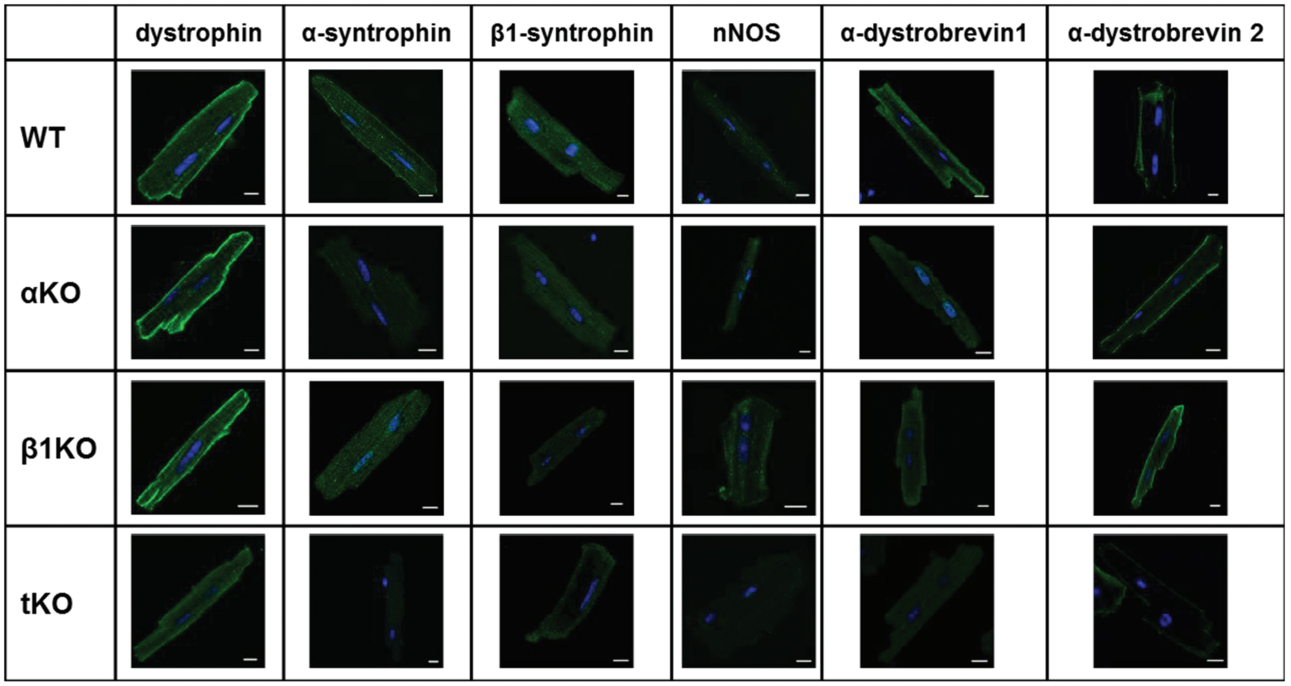

Figure 6. Membrane-localized dystrophin reduced in isolated cardiomyocytes from the tKO. Representative immune staining images for dystrophin-associated proteins on isolated cardiomyocytes from the WT, αKO, β1KO and tKO. Size bar = 10 μm.

current study we generated triple syntrophin knockout (tKO) lacking all three major muscle syntrophin isoforms (α-, β1 and β2-syntrophins) to investigate the overall function of syntrophins on exercise performance and on skeletal and cardiac muscle physiological function *in vivo*.

We generated β1KO mice (see Fig. 1) but observed no overt phenotype in the muscle or NMJ. We then bred β1KO with α/β2 KO mice to ultimately generate the tKO mice. We had previously found that α/β2 KO exercise activity was significantly reduced by ∼50% compared to WT (22), so we tested if the exercise performance of tKO mice was further reduced. At both 6- and 12-month-old tKO, the wheel running activity was dramatically reduced to <25% of 6-month-old WT (see Fig. 2). αKO mice also demonstrated significantly reduced exercise performance compared to WT mice; however values were higher than tKO at 6 months before decreasing to tKO levels at 12 months of age. While we are not able to definitively conclude that exercise activity of tKO is worse than α/β2 KO, since we did not include α/β2 KO in the current study, our findings indicate that the loss of α and β-syntrophins causes a profound loss of voluntary exercise activity and β-syntrophin can partially compensate for the loss of α-syntrophin in younger mice.

Since voluntary exercise activity of tKO was considerably lower than WT mice, we next aimed to determine whether impaired skeletal and/or cardiac muscle function may contribute to this reduced running wheel performance. Previously, we showed that skeletal muscle contractile function and muscle fatigue for the TA muscle were not different between αKO and WT mice (34). Furthermore, muscle force generation for EDL and diaphragm muscles was not different for αKO and WT mice (33). In the current study, *in situ* TA muscle specific force production for tKO mice was 75–80% of WT values at 6 months of age (Fig. 3A) and very near WT values at 15 months of age. It is interesting that the tKO-specific force shows little change with age, perhaps because muscle lacking syntrophin already simulates the aging process. It is also possible that other protein complexes such as the integrin complex partially compensate in the tKO to prevent further reduction of specific force in aged mice. The reduced muscle force production in 6-month-old tKO may contribute to the impaired exercise performance of tKO mice. However, this is a relatively mild effect and it is unlikely that this reduced force production is the sole mechanism leading to reduced exercise performance.

Nevertheless, since there was no observable myopathy in tKO muscles, we sought other possible explanations that may have contributed to the loss of specific force. Differences in fiber-type composition have been shown to contribute to specific force production, with fast glycolytic fibers in rat diaphragm muscle generating the highest and slow fibers the lowest specific force (30). Therefore, we evaluated the fiber-type compositions of muscles from WT, αKO and tKO mice. Although TA muscles from αKO and tKO contained more (8%) type 2A fibers than WT, these relatively small differences seem unlikely to explain the 20–25% reduction of specific force. Therefore, additional studies will be required to determine the mechanism(s) underlying the reduced muscle specific force of tKO mice.

Another possible explanation for the reduced exercise performance could be a reduction in cardiac function. Previous studies have shown that specific mutations in α-syntrophin lead to long QT syndrome and increased risk of sudden infant death syndrome (20); however other cardiomyopathies relating to specific syntrophin isoforms have not been reported. Therefore, we characterized the left ventricular function of cardiac muscle from tKO mice, in comparison with WT and αKO mice, by echocardiography. A key finding of these studies was that tKO mice display significant left ventricular hypertrophy as early as 3 months of age, as shown by increased LV posterior wall thickness (Fig. 5B). Cardiac hypertrophy was also evident in αKO, however in these mice LV wall thickness increased only at 12 months of age. MPI, a global measure of LV systolic and diastolic function (35), was also

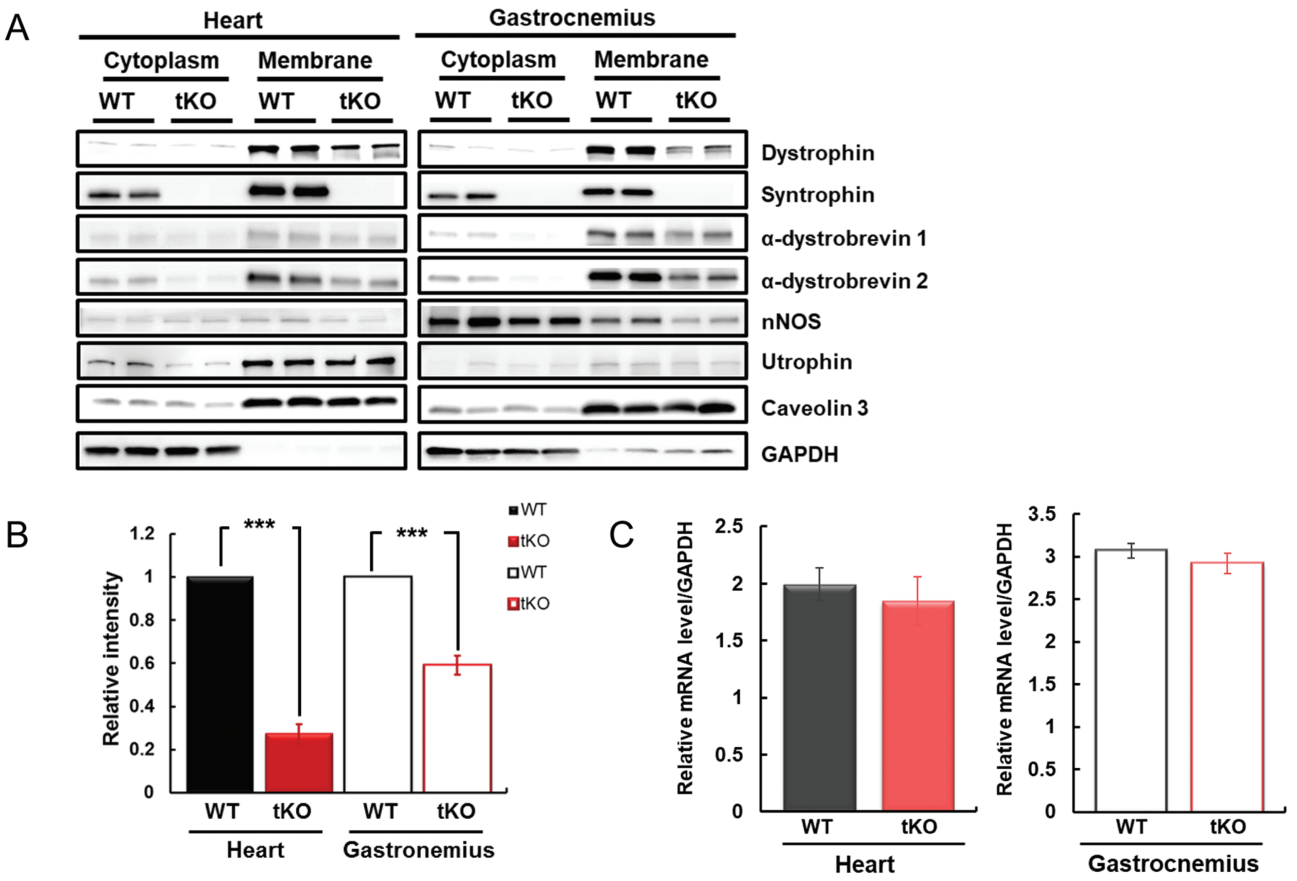

Figure 7. Dystrophin-associated proteins in tKO mice. **(A)** Representative western blots in membrane preparations from the heart and gastrocnemius muscle of WT and tKO mice. **(B)** Relative intensity of dystrophin in membrane preparations from the heart and gastrocnemius of WT and tKO. WT ($n = 16$), tKO ($n = 16$) ***$P < 0.001$ **(C)** Relative mRNA levels for the heart and gastrocnemius of WT and tKO.

significantly different between WT and both αKO and tKO mice (Fig. 5A). Interestingly, common measures of systolic function, EF and FS, were either not different or higher for αKO and tKO mice compared to WT mice. Previous studies have shown that LV hypertrophy can be accompanied by a preserved EF (36). The cellular mechanism(s) by which loss of syntrophins causes LV hypertrophy is currently unclear; however the finding that tKO had greater hypertrophy at a younger age than αKO suggests that β-syntrophins can delay the pathological remodeling. One prominent feature of LV hypertrophy is exercise intolerance (37). Therefore, this pathological feature of tKO cardiac muscle appears to be a likely mechanism that contributes to the poor voluntary exercise performance of these mice. In support of this concept, the exercise activity levels of the αKO mice were indistinguishable from tKO mice at 12 months of age, at which time there was a marked increase in the LV wall thickness of αKO mice. Therefore, our data suggest that cardiac dysfunction is likely to be a major underlying cause of the impaired exercise capacity of both αKO and tKO mice. Future studies will be aimed at determining the cellular mechanisms by which loss of syntrophins lead to cardiac hypertrophy and dysfunction, and the specific roles provided by α and β-syntrophins in these processes.

Syntrophins bind to dystrophin at the sarcolemma and serve as a scaffold for a number of important signaling proteins, including nNOSμ which plays an important role in the physiological function of skeletal muscle (12,38). While the loss of dystrophin leads to reduced expression and targeting of syntrophin at the sarcolemma, the reciprocal role of syntrophins on dystrophin expression and localization has not been previously explored. Here, we show for the first time in tKO mice that loss of both α and β syntrophins significantly reduces dystrophin expression and sarcolemmal targeting in both skeletal and cardiac muscle. The levels of dystrophin reduction (to 59 and 27% of WT levels in skeletal and cardiac muscle) in the tKO mice are not sufficient to produce an overt histopathology but do affect muscle function. Since dystrophin transcript levels were normal, this suggests that the attenuated dystrophin protein expression in tKO muscles is caused by a post-transcriptional mechanism. Two obvious possibilities are that syntrophins stabilize dystrophin at the sarcolemma, reducing turnover and increasing lifetime or that syntrophins assist in targeting dystrophin to the sarcolemma. We have previously posed the same possibilities to explain how α-syntrophin affects utrophin's location at the NMJ post-synaptic membrane. In the αKO, utrophin is not present at the NMJ despite presence of the mRNA as levels similar to control. Dystrophin family members are not the only proteins that depend on syntrophin for membrane localization. Syntrophin is required for expression of α1D-adrenergic receptor at the membrane (39) and for normal density of cardiac sodium channels (40). It is notable that even though dystrophin expression is reduced by up to 59% of normal, no muscle myopathy is observed in these mice. This level of dystrophin expression appears sufficient for the prevention of a dystrophic phenotype.

In summary, our results provide new insights into the role of syntrophins in skeletal and cardiac muscle function and whole body exercise performance. As such, these findings highlight important new functions of syntrophins in striated muscle and indicate that further research is warranted to understand how syntrophins regulate specific cellular pathways. A full understanding of the functions of syntrophins may lead to new therapeutic approaches for treating neuromuscular and cardiac diseases.

Materials and Methods

β1-syntrophin null mice generation

We generated a targeting construct containing 5.7 kb of sequence 5′ and 1.1 kb of sequence 3′ of the first exon of mouse β1-syntrophin in a pSP72 plasmid containing a p-loxP-2FRT-PGK neo cassette. A second loxP site was introduced 3.9 kb upstream of exon 1 (Fig. 1). This construct was electroporated into mouse embryonic stem (ES) cells and homologous recombinant clones identified by PCR and confirmed by southern blot. After removal of the neo cassette, positive ES cells were injected into blastocyst of C3H/C57bl6 F1 hybrids (University of Washington, Transgenic Resources Program). Resulting 'floxed' mice were bred with mice expressing Cre recombinase under control of the CMV promoter (Jackson Labs, Bar Harbor, ME) to produce $Sntb1^{+/-}$ mice that were subsequently crossed to generate $Sntb1^{-/-}$ mice. $Sntb1^{-/-}$ mice were bred onto the C57bl6 background (WT) for >10 generations. All experimental procedures were approved by the Institutional Animal Care and Use Committee at the University of Washington.

Antibodies

The antibodies for dystrophin, α-syntrophin, β1-syntrophin, α-dystrobrevin1 and α-dystrobrevin2 were described previously (19). We used commercial antibodies for Caveolin-3 (BD Biosciences, Franklin Lakes, NJ), GAPDH (Millipore, Burlington, MA) and nNOS (Invitrogen). The antibodies for the fiber-type analysis including myosin heavy chain 1, myosin heavy chain 2X, myosin heavy chain 2A and myosin heavy chain 2B were from Developmental Studies Hybridoma bank.

Voluntary wheel running

WT, αKO and tKO mice were individually caged at the indicated ages (6 or 12–15 months of age). Voluntary wheel running was measured with a single activity wheel system (Lafayette Instrument Company, Lafayette, IN). The wheel revolutions were recorded for 14 days, with activity data (wheel revolutions) downloaded every 1 h and analyzed using the activity wheel monitoring software. The number of wheel revolutions per day was calculated by averaging the revolutions over 14 days and data was expressed as a percentage of WT values.

Skeletal muscle contractile function

Skeletal muscle contractile function was determined as described in (41,42). Briefly, mice were anesthetized and laid on the heated 37°C platform during experiments. The distal tendon of the TA muscle was isolated and attached to the lever of a servomotor (Aurora Scientific, ON, Canada). The TA muscle contraction was initiated by stimulating the sciatic nerve using platinum electrodes. The optimum length (Lo) was measured by constructing an isometric length-force relationship over a range of muscle lengths, with the muscle stimulated at each length with 120 Hz stimulation (200 ms duration) every 90 sec. A force-frequency curve was then measured using 80, 120 and 200 Hz stimulation. The isometric force at each frequency was normalized to the cross-section area [(Lo × density)/mass] to calculate the specific force (mN/mm^2).

Echocardiography

Echocardiography was performed using the Vevo 2100 Imaging System (FUJI FILM Visual Sonic, Tokyo, Japan) on WT, αKO and tKO mice at the ages of 3, 6 and 12 months. Mice were anaesthetized with 5% isoflurane mixed with O_2. Mice were then placed on a heated platform, and anesthesia was maintained by 1.5% isoflurane. Since isoflurane depresses heart rate, dobutamine was injected I.P. (2 mg/kg) to restore heart rate to a more normal physiological range of between 500 and 650 bpm. For assessing diastolic function (DTI), early diastolic velocity peak (E′) and late diastolic peak (A′) were measured along the short axis view using Tissue Doppler Mode. The DTI was then determined from the ratio of E′/A′ and values above 1.0 were considered normal. The MPI, a universal measure of left ventricular systolic and diastolic function, was determined using Pulse-Wave Doppler Mode. For calculating MPI, aortic ejection time and the non-flow time of the left ventricle were measured. To assess systolic function, EF and FS were calculated by measuring the following parameters: intraventricular septum thickness in diastole, LVPW;d, left ventricular diameter in diastole and left ventricular internal diameter in systolic. These values were measured along the parasternal short axis view in Motion mode (M-mode).

Western blotting

Liver, skeletal and cardiac muscle tissue were dissected and prepared for western blotting as previously described by our laboratory (19). Briefly, frozen tissues were lysed in homogenization buffer (HB) containing 2 mM sodium phosphate, 0.08 M NaCl, 1 mM EDTA, pH 7.8, 1 mM PMSF, phosphatase inhibitor (Roche, Basel, Switzerland) and protease inhibitor (Thermo Scientific, Waltham, MA), using a tissue homogenizer (Kinematica Polytron, Lucerne, Switzerland). Samples were then centrifuged at 12 000 x g for 10 min at 4°C. To prepare the membrane fraction, pellets were resuspended in HB with 1% Triton X-100 for 1 h on ice and then centrifuged at 12 000 x g for 10 min at 4°C. Protein concentration was determined by bicinchoninic acid assay reagent (Pierce). Equal amounts of protein were loaded into a 4–15% polyacrylamide gel (Biorad) and then transferred onto a polyvinylidene difluoride (PVDF) membrane (Millipore). The membranes were blocked with 5% skim milk in TBS containing 0.1% Tween (TBST) and incubated with indicated primary antibodies overnight at 4°C, followed by horseradish peroxidase (HRP)-conjugated secondary antibodies for 1 h at room temperature. Protein bands were detected using enhanced chemiluminescence (Pierce) and a FluroChem M imager (Protein Simple, San Jose, CA). The band intensity was determined by densitometry using Image J.

Cardiomyocyte isolation

The cardiomyocytes isolation was performed using the Langendorff perfusion apparatus as previously described (43,44). Briefly, the excised heart was rinsed with ice cold Digestion Buffer (DB) containing 130 mM NaCl, 5 mM KCl, 3 mM Pyruvic acid, 25 mM HEPES, 0.5 mM $MgCl_2$, 0.33 mM NaH_2PO_4 and 22 mM Glucose. The aorta was cannulated and connected to the Langendorff perfusion system. The heart was perfused with DB until all blood was removed and then the tissue was digested in DB containing protease type XIV (Worthington, Lakewood, NJ) (0.04 mg/ml) and collagenase Type 2 (Sigma, St. Louis, MO) (1.0 mg/ml) for 10 min. The ventricles were cut away from the cannula and placed in 0.04 mg/ml protease and 1.2 mg/ml collagenase dissolved in DB. The isolated cardiomyocytes were precipitated in neutralization buffer consisting of DB with 0.25 mM of $CaCl_2$ and 10 mg/ml of BSA for 25 min then stored in Tyrode's solution. A small aliquot of cardiomyocytes (50–100 ul) was then placed on glass slides and allowed sufficient time to adhere to the glass (30 min at 37°C).

Immunohistochemistry

For hematoxylin and eosin (H&E) staining, the sections were fixed in cold methanol for 10 min and then stained by standard hematoxylin eosin procedures (41). For muscle fiber typing, TA and diaphragm tissues were dissected from mice at 12–15 months of age, placed in Tissue Tek OCT and snap frozen in isopentane cooled in liquid nitrogen. Cryostat sections (10 µm) were immunolabeled with the indicated primary antibody as described (42) then treated with Alexa Fluor 488 or 555 (ThermoFisher) conjugated secondary antibodies and DAPI for 45 min at room temperature. Samples were mounted with Slowfade Gold antifade reagent (ThermoFisher). The H&E and fiber-typing images were obtained with a Zeiss Axioscop 2 fluorescent microscope and analyzed using Image J. For Cardiomyocyte immunostaining, cells were fixed on glass slides and stained as per the protocol used for muscle fiber typing. Images of cardiomyocytes were obtained using a Zeiss LSM510 confocal microscope (W.M. Keck Center for Advanced Studies in Neural Signaling at the University of Washington).

Supplementary Material

Supplementary Material is available at *HMG* online.

Funding

NIH (NS33145 to S.C.F.); University of Washington Royalty Research Fund (to M.E.A.); National Heart, Lung, and Blood Institute Cardiovascular Training (T32HL007828 to M.J.K.); and by the National Research Foundation of Korea grant funded by the Korea Government (NRF-2011-357-C00104 to M.J.K.).

References

1. Adams, M.E., Dwyer, T.M., Dowler, L.L., White, R.A. and Froehner, S.C. (1995) Mouse alpha 1- and beta 2-syntrophin gene structure, chromosome localization, and homology with a discs large domain. *J. Biol. Chem.*, **270**, 25859–25865.
2. Ahn, A.H. and Kunkel, L.M. (1995) Syntrophin binds to an alternatively spliced exon of dystrophin. *J. Cell Biol.*, **128**, 363–371.
3. Dwyer, T.M. and Froehner, S.C. (1995) Direct binding of Torpedo syntrophin to dystrophin and the 87 kDa dystrophin homologue. *FEBS Lett.*, **375**, 91–94.
4. Yang, B., Jung, D., Rafael, J.A., Chamberlain, J.S. and Campbell, K.P. (1995) Identification of alpha-syntrophin binding to syntrophin triplet, dystrophin, and utrophin. *J. Biol. Chem.*, **270**, 4975–4978.
5. Suzuki, A., Yoshida, M. and Ozawa, E. (1995) Mammalian alpha 1- and beta 1-syntrophin bind to the alternative splice-prone region of the dystrophin COOH terminus. *J. Cell Biol.*, **128**, 373–381.
6. Alessi, A., Bragg, A.D., Percival, J.M., Yoo, J., Albrecht, D.E., Froehner, S.C. and Adams, M.E. (2006) gamma-Syntrophin scaffolding is spatially and functionally distinct from that of the alpha/beta syntrophins. *Exp. Cell Res.*, **312**, 3084–3095.
7. Neely, J.D., Amiry-Moghaddam, M., Ottersen, O.P., Froehner, S.C., Agre, P. and Adams, M.E. (2001) Syntrophin-dependent expression and localization of Aquaporin-4 water channel protein. *Proc. Natl. Acad. Sci. USA*, **98**, 14108–14113.
8. Gee, S.H., Madhavan, R., Levinson, S.R., Caldwell, J.H., Sealock, R. and Froehner, S.C. (1998) Interaction of muscle and brain sodium channels with multiple members of the syntrophin family of dystrophin-associated proteins. *J. Neurosci.*, **18**, 128–137.
9. Williams, J.C., Armesilla, A.L., Mohamed, T.M., Hagarty, C.L., McIntyre, F.H., Schomburg, S., Zaki, A.O., Oceandy, D., Cartwright, E.J., Buch, M.H. *et al.* (2006) The sarcolemmal calcium pump, alpha-1 syntrophin, and neuronal nitric-oxide synthase are parts of a macromolecular protein complex. *J. Biol. Chem.*, **281**, 23341–23348.
10. Brenman, J.E., Chao, D.S., Gee, S.H., McGee, A.W., Craven, S.E., Santillano, D.R., Wu, Z., Huang, F., Xia, H., Peters, M.F. *et al.* (1996) Interaction of nitric oxide synthase with the postsynaptic density protein PSD-95 and alpha1-syntrophin mediated by PDZ domains. *Cell*, **84**, 757–767.
11. Hashida-Okumura, A., Okumura, N., Iwamatsu, A., Buijs, R.M., Romijn, H.J. and Nagai, K. (1999) Interaction of neuronal nitric-oxide synthase with alpha1-syntrophin in rat brain. *J. Biol. Chem.*, **274**, 11736–11741.
12. Adams, M.E., Odom, G.L., Kim, M.J., Chamberlain, J.S. and Froehner, S.C. (2018) Syntrophin binds directly to multiple spectrin-like repeats in dystrophin and mediates binding of nNOS to repeats 16-17. *Hum. Mol. Genet.*, **27**, 2978–2985.
13. Hasegawa, M., Cuenda, A., Spillantini, M.G., Thomas, G.M., Buee-Scherrer, V., Cohen, P. and Goedert, M. (1999) Stress-activated protein kinase-3 interacts with the PDZ domain of alpha1-syntrophin. A mechanism for specific substrate recognition. *J. Biol. Chem.*, **274**, 12626–12631.
14. Lumeng, C., Phelps, S., Crawford, G.E., Walden, P.D., Barald, K. and Chamberlain, J.S. (1999) Interactions between beta 2-syntrophin and a family of microtubule-associated serine/threonine kinases. *Nat. Neurosci.*, **2**, 611–617.
15. Allen, D.G., Whitehead, N.P. and Froehner, S.C. (2016) Absence of dystrophin disrupts skeletal muscle signaling: roles of Ca2+, reactive oxygen species, and nitric oxide in the development of muscular dystrophy. *Physiol. Rev.*, **96**, 253–305.
16. Chockalingam, P.S., Gee, S.H. and Jarrett, H.W. (1999) Pleckstrin homology domain 1 of mouse alpha 1-syntrophin binds phosphatidylinositol 4,5-bisphosphate. *Biochemistry*, **38**, 5596–5602.
17. Peters, M.F., Kramarcy, N.R., Sealock, R. and Froehner, S.C. (1994) Beta-2-syntrophin - localization at the neuro-

muscular-junction in skeletal-muscle. *Neuroreport*, **5**, 1577–1580.
18. Adams, M.E., Butler, M.H., Dwyer, T.M., Peters, M.F., Murnane, A.A. and Froehner, S.C. (1993) Two forms of mouse syntrophin, a 58 kd dystrophin-associated protein, differ in primary structure and tissue distribution. *Neuron*, **11**, 531–540.
19. Peters, M.F., Adams, M.E. and Froehner, S.C. (1997) Differential association of syntrophin pairs with the dystrophin complex. *J. Cell Biol.*, **138**, 81–93.
20. Cheng, J., Van Norstrand, D.W., Medeiros-Domingo, A., Valdivia, C., Tan, B.H., Ye, B., Kroboth, S., Vatta, M., Tester, D.J., January, C.T. *et al.* (2009) Alpha1-syntrophin mutations identified in sudden infant death syndrome cause an increase in late cardiac sodium current. *Circ. Arrhythm. Electrophysiol.*, **2**, 667–676.
21. Adams, M.E., Kramarcy, N., Krall, S.P., Rossi, S.G., Rotundo, R.L., Sealock, R. and Froehner, S.C. (2000) Absence of alpha-syntrophin leads to structurally aberrant neuromuscular synapses deficient in utrophin. *J. Cell Biol.*, **150**, 1385–1398.
22. Adams, M.E., Kramarcy, N., Fukuda, T., Engel, A.G., Sealock, R. and Froehner, S.C. (2004) Structural abnormalities at neuromuscular synapses lacking multiple syntrophin isoforms. *J. Neurosci.*, **24**, 10302–10309.
23. Ueda, K., Valdivia, C., Medeiros-Domingo, A., Tester, D.J., Vatta, M., Farrugia, G., Ackerman, M.J. and Makielski, J.C. (2008) Syntrophin mutation associated with long QT syndrome through activation of the nNOS-SCN5A macromolecular complex. *Proc. Natl. Acad. Sci. USA*, **105**, 9355–9360.
24. Wu, G., Ai, T., Kim, J.J., Mohapatra, B., Xi, Y., Li, Z., Abbasi, S., Purevjav, E., Samani, K., Ackerman, M.J. *et al.* (2008) alpha-1-syntrophin mutation and the long-QT syndrome: a disease of sodium channel disruption. *Circ. Arrhythm. Electrophysiol.*, **1**, 193–201.
25. Choi, J.I., Wang, C., Thomas, M.J. and Pitt, G.S. (2016) alpha1-syntrophin variant identified in drug-induced long QT syndrome increases late sodium current. *PLoS One*, **11**, e0152355.
26. Cafferkey, A. and McMahon, C. (2018) Successful treatment of refractory cardiac arrest with beta-blockade and extracorporeal life support in a pediatric patient with catecholaminergic polymorphic ventricular tachycardia: a case report. *A A Pract.*, **11**, 63–67.
27. Johnson, E.K., Zhang, L., Adams, M.E., Phillips, A., Freitas, M.A., Froehner, S.C., Green-Church, K.B. and Montanaro, F. (2012) Proteomic analysis reveals new cardiac-specific dystrophin-associated proteins. *PLoS One*, **7**, e43515.
28. Schiaffino, S., Gorza, L., Sartore, S., Saggin, L., Ausoni, S., Vianello, M., Gundersen, K. and Lomo, T. (1989) Three myosin heavy chain isoforms in type 2 skeletal muscle fibres. *J. Muscle Res. Cell Motil.*, **10**, 197–205.
29. Schiaffino, S. and Reggiani, C. (1994) Myosin isoforms in mammalian skeletal muscle. *J. Appl. Physiol. (1985)*, **77**, 493–501.
30. Geiger, P.C., Cody, M.J., Macken, R.L. and Sieck, G.C. (2000) Maximum specific force depends on myosin heavy chain content in rat diaphragm muscle fibers. *J. Appl. Physiol. (1985)*, **89**, 695–703.
31. Strakova, J., Dean, J.D., Sharpe, K.M., Meyers, T.A., Odom, G.L. and Townsend, D. (2014) Dystrobrevin increases dystrophin's binding to the dystrophin-glycoprotein complex and provides protection during cardiac stress. *J. Mol. Cell. Cardiol.*, **76**, 106–115.
32. Thomas, G.D., Shaul, P.W., Yuhanna, I.S., Froehner, S.C. and Adams, M.E. (2003) Vasomodulation by skeletal muscle-derived nitric oxide requires alpha-syntrophin-mediated sarcolemmal localization of neuronal Nitric oxide synthase. *Circ. Res.*, **92**, 554–560.
33. Yokota, T., Miyagoe-Suzuki, Y., Ikemoto, T., Matsuda, R. and Takeda, S. (2014) alpha1-syntrophin-deficient mice exhibit impaired muscle force recovery after osmotic shock. *Muscle Nerve*, **49**, 728–735.
34. Percival, J.M., Anderson, K.N., Huang, P., Adams, M.E. and Froehner, S.C. (2010) Golgi and sarcolemmal neuronal NOS differentially regulate contraction-induced fatigue and vasoconstriction in exercising mouse skeletal muscle. *J. Clin. Invest.*, **120**, 816–826.
35. Arnlov, J., Ingelsson, E., Riserus, U., Andren, B. and Lind, L. (2004) Myocardial performance index, a Doppler-derived index of global left ventricular function, predicts congestive heart failure in elderly men. *Eur. Heart J.*, **25**, 2220–2225.
36. Heinzel, F.R., Hohendanner, F., Jin, G., Sedej, S. and Edelmann, F. (2015) Myocardial hypertrophy and its role in heart failure with preserved ejection fraction. *J. Appl. Physiol. (1985)*, **119**, 1233–1242.
37. Lam, C.S., Grewal, J., Borlaug, B.A., Ommen, S.R., Kane, G.C., McCully, R.B. and Pellikka, P.A. (2010) Size, shape, and stamina: the impact of left ventricular geometry on exercise capacity. *Hypertension*, **55**, 1143–1149.
38. Percival, J.M. (2011) nNOS regulation of skeletal muscle fatigue and exercise performance. *Biophys. Rev.*, **3**, 209–217.
39. Chen, Z., Hague, C., Hall, R.A. and Minneman, K.P. (2006) Syntrophins regulate alpha1D-adrenergic receptors through a PDZ domain-mediated interaction. *J. Biol. Chem.*, **281**, 12414–12420.
40. Shy, D., Gillet, L., Ogrodnik, J., Albesa, M., Verkerk, A.O., Wolswinkel, R., Rougier, J.S., Barc, J., Essers, M.C., Syam, N. *et al.* (2014) PDZ domain-binding motif regulates cardiomyocyte compartment-specific NaV1.5 channel expression and function. *Circulation*, **130**, 147–160.
41. Whitehead, N.P., Kim, M.J., Bible, K.L., Adams, M.E. and Froehner, S.C. (2015) A new therapeutic effect of simvastatin revealed by functional improvement in muscular dystrophy. *Proc. Natl. Acad. Sci. USA*, **112**, 12864–12869.
42. Rebolledo, D.L., Kim, M.J., Whitehead, N.P., Adams, M.E. and Froehner, S.C. (2016) Sarcolemmal targeting of nNOSmu improves contractile function of mdx muscle. *Hum. Mol. Genet.*, **25**, 158–166.
43. Shioya, T. (2007) A simple technique for isolating healthy heart cells from mouse models. *J. Physiol. Sci.*, **57**, 327–335.
44. Drum, B.M.L., Dixon, R.E., Yuan, C., Cheng, E.P. and Santana, L.F. (2014) Cellular mechanisms of ventricular arrhythmias in a mouse model of Timothy syndrome (long QT syndrome 8). *J. Mol. Cell. Cardiol.*, **66**, 63–71.